

## Electronic Supplementary Information (ESI)

to the manuscript:

### Synthesis, biological evaluation and Metadynamics simulations of novel N-Methyl $\beta$ -sheet breaker peptides as inhibitors of the Alzheimer's $\beta$ -amyloid fibrillogenesis

Federica Moraca,<sup>a,b,§</sup> Ilaria Vespoli,<sup>c,§</sup> Domenico Mastroianni,<sup>d</sup> Vincenzo Piscopo,<sup>e</sup> Rosa Gaglione,<sup>d,f</sup> Angela Arciello,<sup>d,f</sup> Mauro De Nisco,<sup>g,\*</sup> Severina Pacifico,<sup>e</sup> Bruno Catalanotti,<sup>a</sup> and Silvana Pedatella<sup>d</sup>

<sup>a</sup> Department of Pharmacy, University of Napoli Federico II, I-80131 Napoli, Italy.

<sup>b</sup> Net4Science Academic Spin-Off, University "Magna Græcia" of Catanzaro, 88100 Catanzaro, Italy.

<sup>c</sup> Institute of Organic Chemistry and Biochemistry of the Czech Academy of Sciences, CZ-16610 Prague, Czech Republic.

<sup>d</sup> Department of Chemical Sciences, University of Napoli Federico II, I-80126, Napoli, Italy.

<sup>e</sup> Department of Environmental, Biological and Pharmaceutical Sciences and Technologies, University of Campania "Luigi Vanvitelli", I-81100 Caserta, Italy.

<sup>f</sup> Istituto Nazionale di Biostrutture e Biosistemi (INBB), I-80145 Roma, Italy.

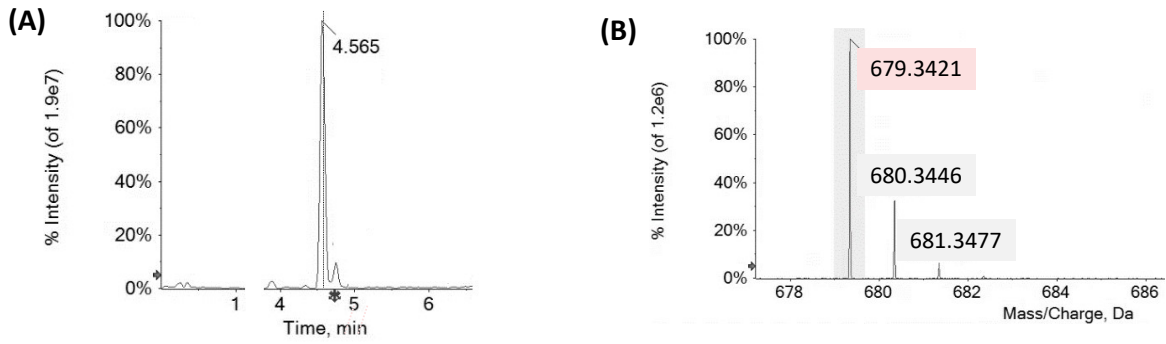
<sup>g</sup> Department of Sciences, University of Basilicata, I-85100 Potenza, Italy.

<sup>§</sup> F.M., and I.V. have contributed equally to this work and share the first authorship.

\* Corresponding author: mauro.denisco@unibas.it (M.D.N.)

Contents	Pages
Figure S1	S3
Figure S2	S3
Figure S3	S4
Figure S4	S4
Figure S5	S5
Figure S6	S5
Figure S7	S6
Figure S8	S6
Figure S9	S7
Table S1	S8-S11
Figure S10	S11
Text S1	S11
Text S2	S12
Figure S11	S12
Figure S12	S12
Figure S13	S13
Figure S14	S13-S14
Figure S15	S14-S15
Table S2	S15
Table S3	S16
Table S4	S16
Table S5	S17
Figure S16	S17
Figure S17	S18
Text S3	S18
Figure S18	S19

Figure S19	S19
Figure S20	S19
Figure S21	S20
Figure S22	S20
Figure S23	S20
Figure S24	S21
Figure S25	S21
Figure S26	S22
Figure S27	S22
Figure S28-S29	S23
Figure S30-S31	S24
Figure S32	S25
References	S26



$C_{35}H_{46}N_6O_8$ ;  $[M+H]^+$  calcd.  $m/z$  679.3450, error ppm -4.3

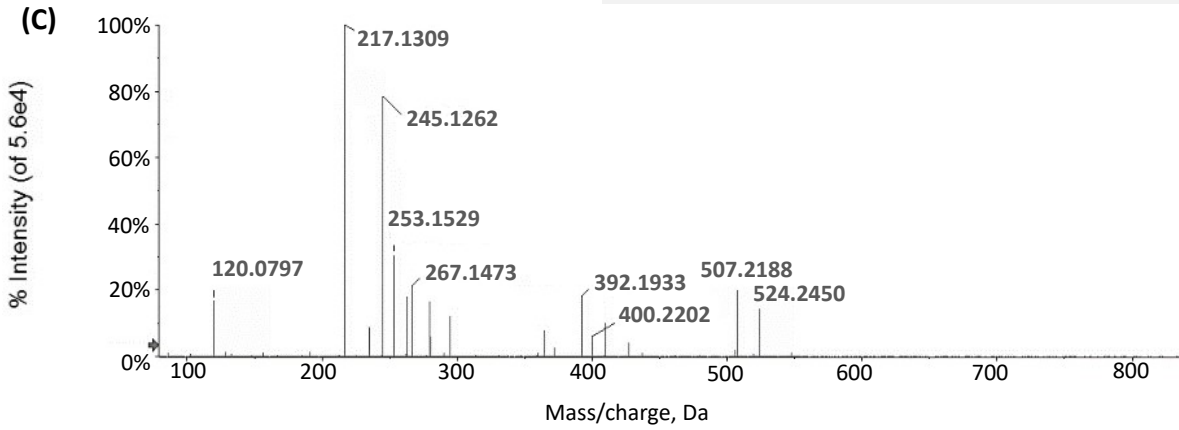
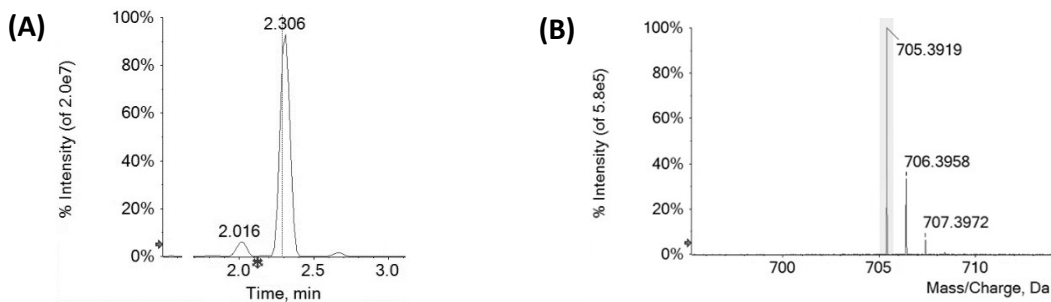


**Figure S1.** UHPLC-MS data for peptide 1. (A) Total Ion Chromatogram (TIC); (B) TOF-MS spectrum; (C) TOF-MS/MS spectrum.



$C_{35}H_{52}N_8O_9$ ;  $[M+H]^+$  calcd.  $m/z$  705.3930, error ppm -1.6

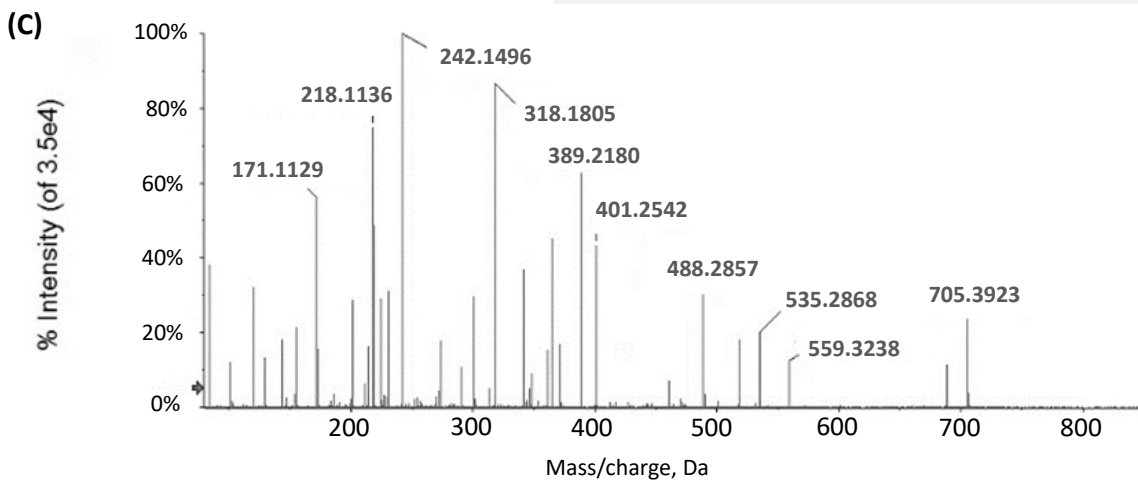


**Figure S2.** UHPLC-MS data for peptide **2**. (A) Total Ion Chromatogram (TIC); (B) TOF-MS spectrum; and (C) TOF-MS/MS spectrum.

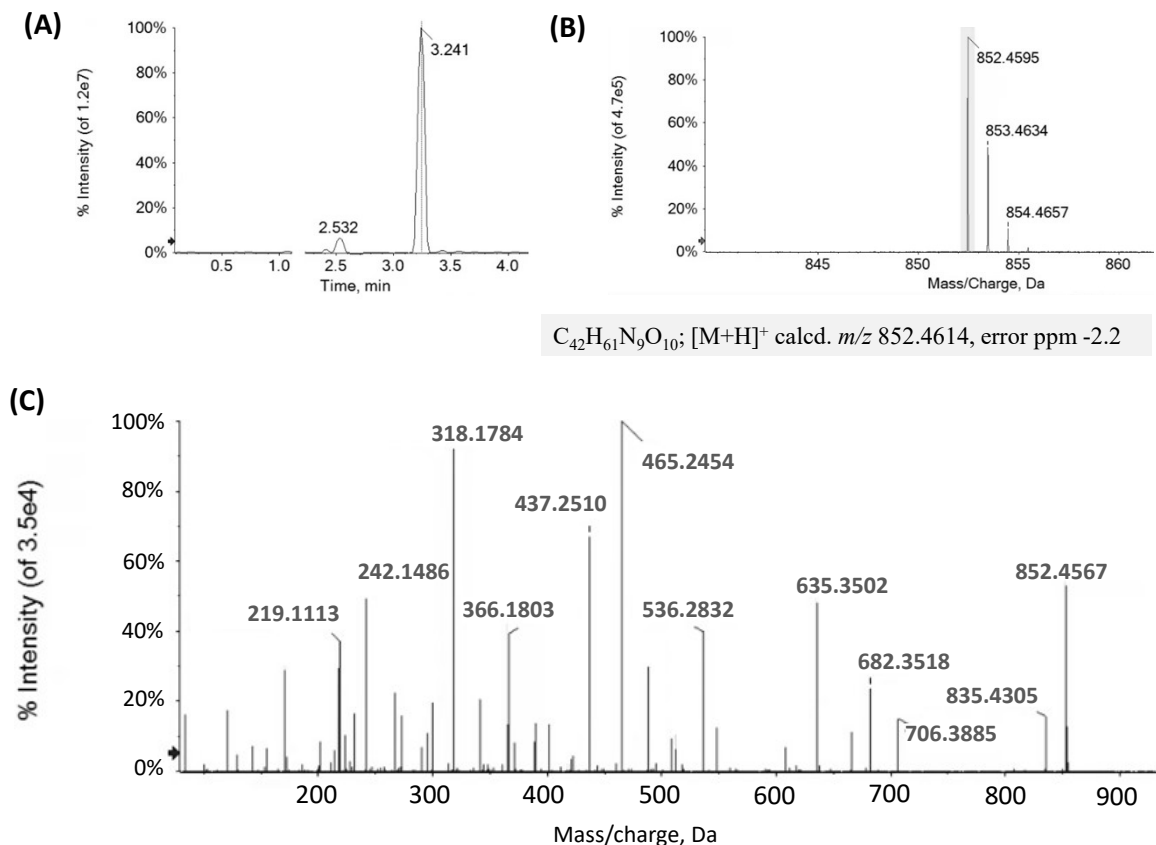


**Figure S3.** UHPLC-MS data for peptide **3**. (A) Total Ion Chromatogram (TIC); (B) TOF-MS spectrum; and (C) TOF-MS/MS spectrum.

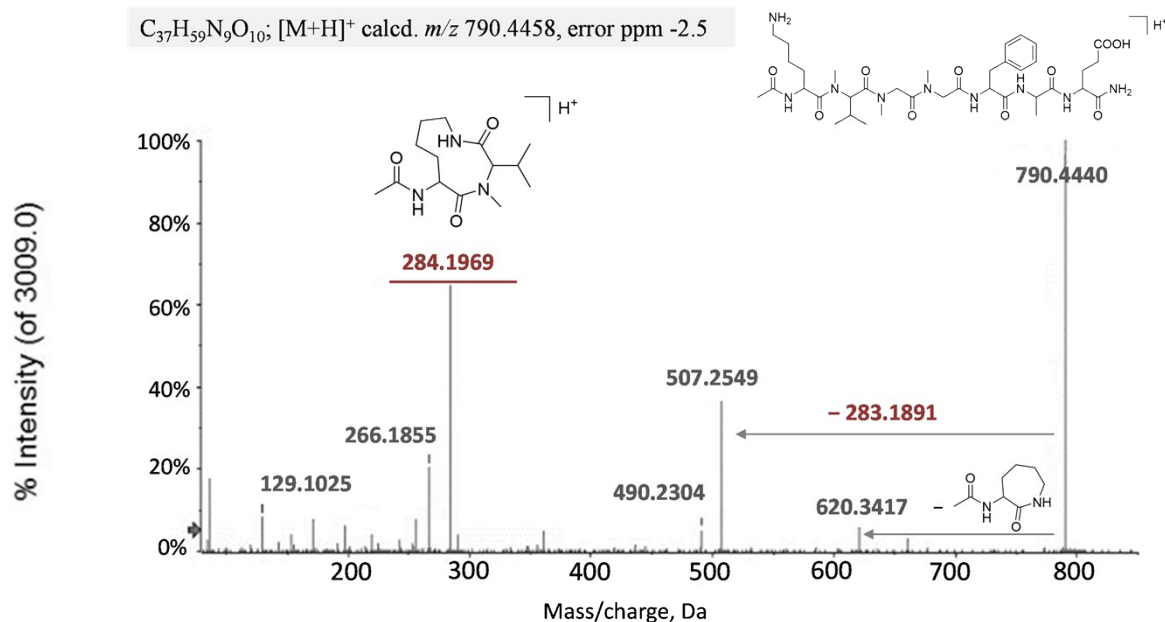
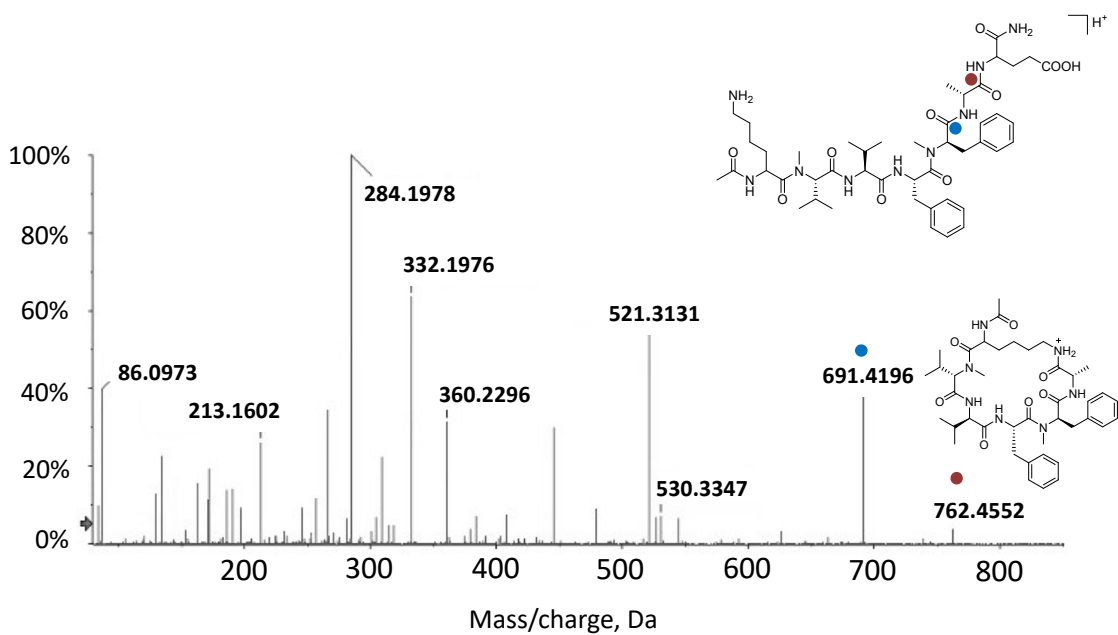


**Figure S4.** TOF-MS data and TOF-MS/MS spectrum for peptide **4**.



$C_{46}H_{69}N_9O_{10}$ ;  $[M+H]^+$  calcd.  $m/z$  908.5263, error ppm +2.5

**Figure S5.** TOF-MS data and TOF-MS/MS spectrum for peptide 5.

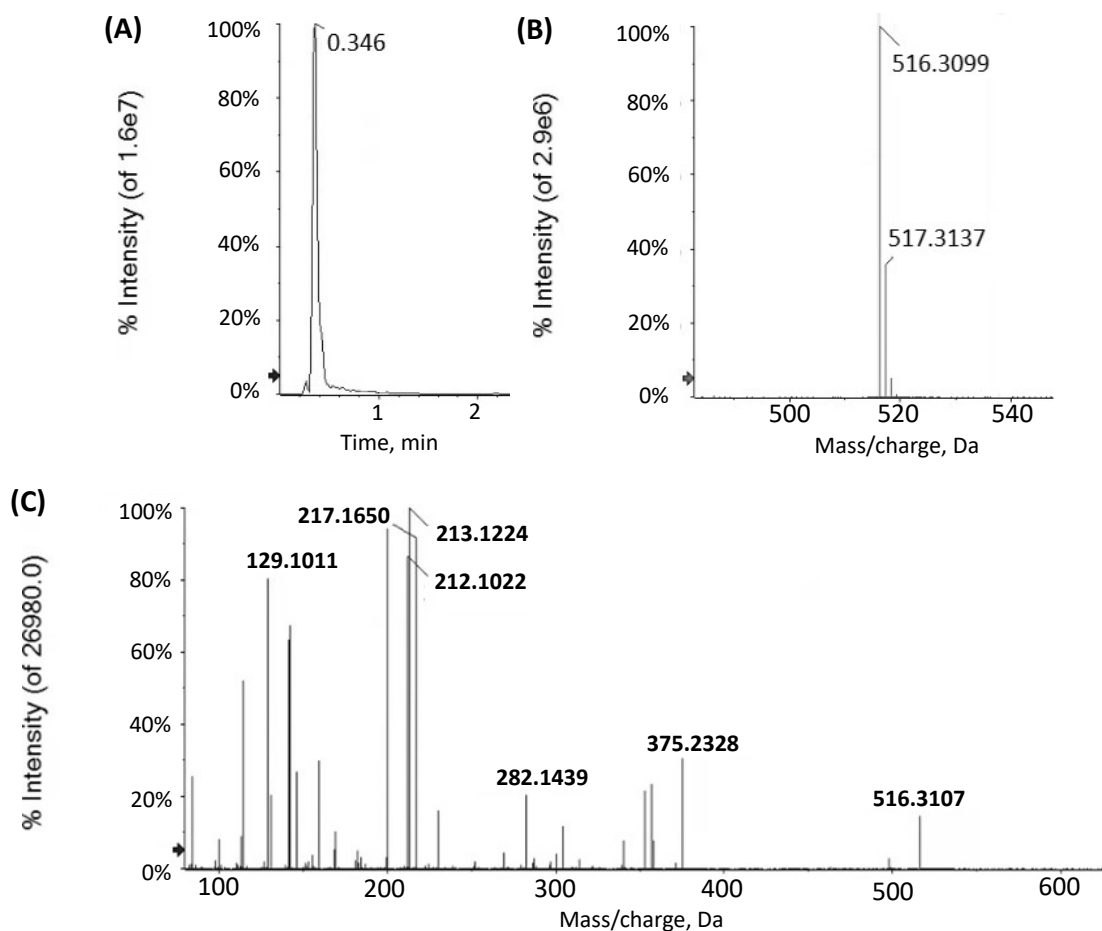


**Figure S6.** UHPLC-MS data for peptide 6. (A) Total Ion Chromatogram (TIC); (B) TOF-MS spectrum; and (C) TOF-MS/MS spectrum.

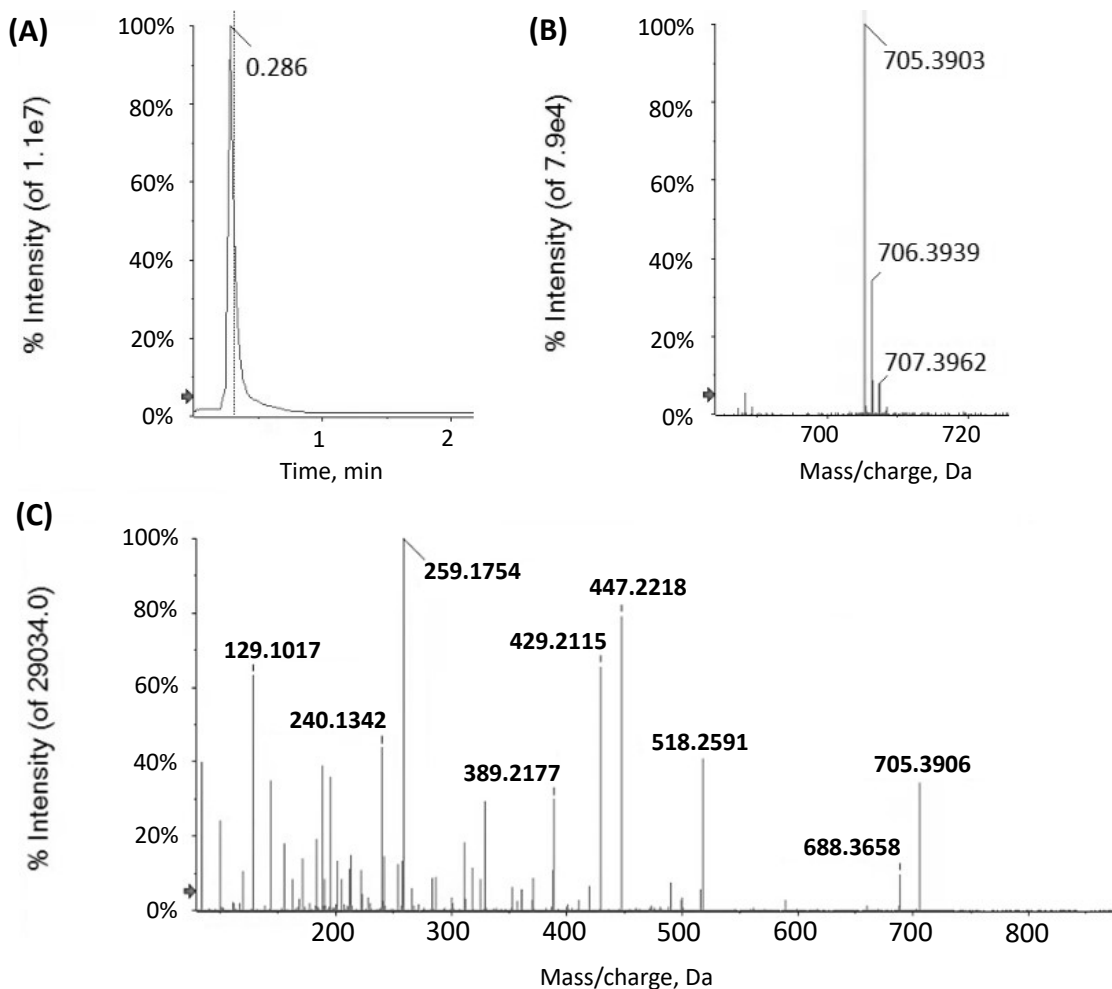
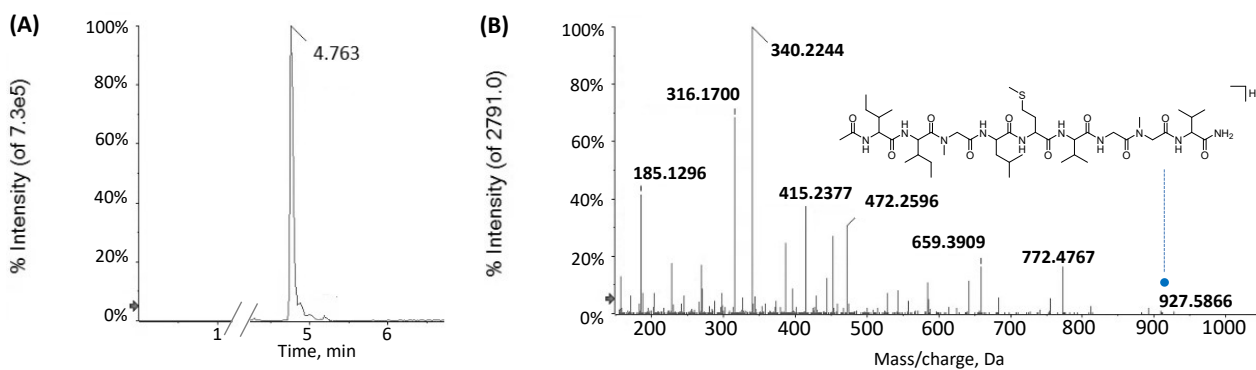
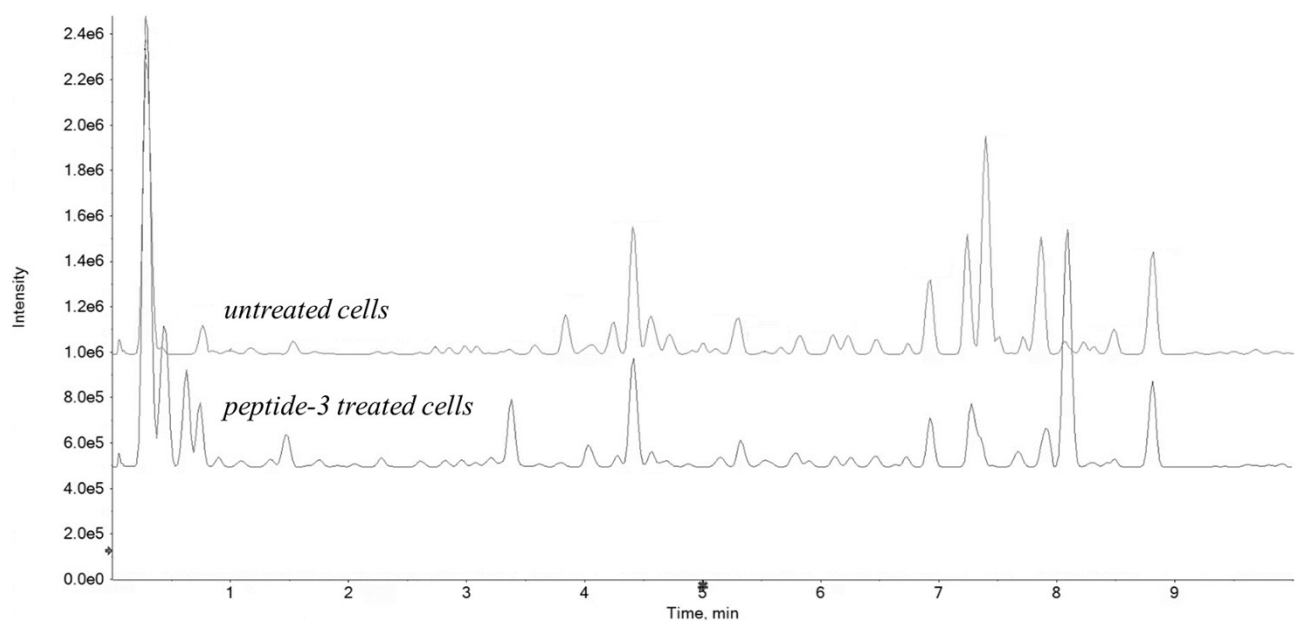


**Figure S7.** UHPLC-MS data for peptide **7**. **(A)** Total Ion Chromatogram (TIC); **(B)** TOF-MS spectrum; and **(C)** TOF-MS/MS spectrum.



$C_{43}H_{78}N_{10}O_{10}S$ ;  $[M+H]^+$  calcd.  $m/z$  927.5686, error ppm  $-0.9$

**Figure S8.** **(A)** Total Ion Chromatogram (TIC); and **(B)** TOF-MS/MS spectrum for peptide **8**.

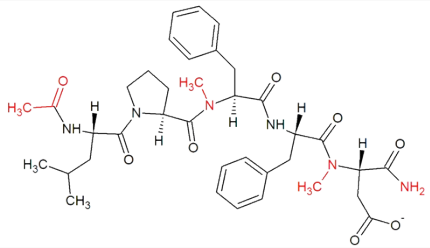
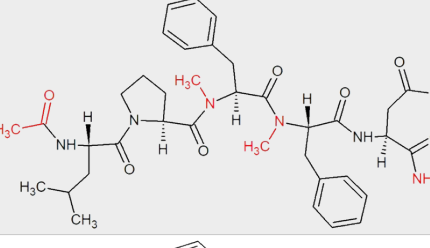
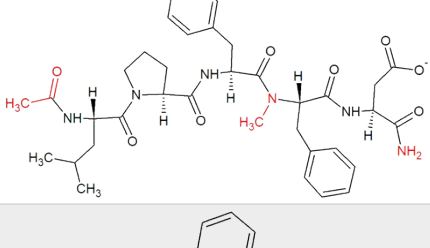
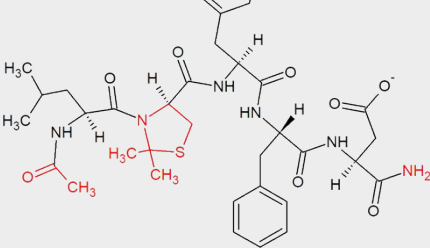
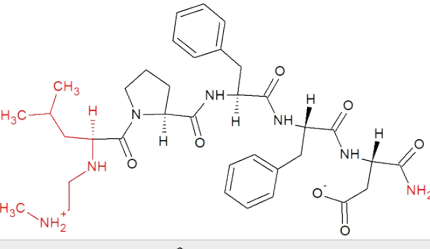
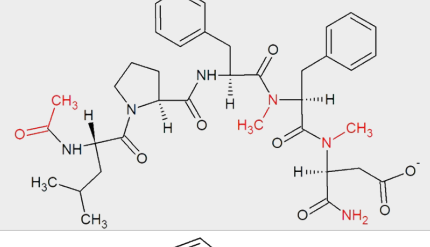
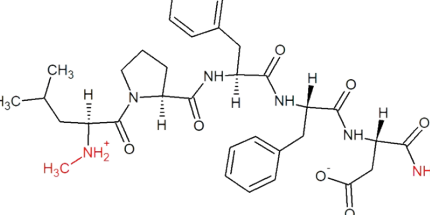


**Figure S9.** Representative Total Ion Current (TIC) chromatograms of extracts from treated and untreated cell pellets.

**Table S1.** 2D structures of the known BSB peptides collected from the work of Adessi et. al. 2003 [1].

Name	Sequence	Active/Inactive/Decoys	2D Structure
<i>iAβ5p</i>	Ac-LPFFD-NH <sub>2</sub>	Active	
<i>iAβ5p-C3</i>	(NMe)Sar-LPFFD-NH <sub>2</sub>	Active	
<i>iAβ5p-B1</i>	Ac-LP-(αMe)F-(αMe)FD-NH <sub>2</sub>	Active	
<i>iAβ5p-C1</i>	(H)-LPFFD-NH <sub>2</sub>	Active	
<i>iAβ5p-C2</i>	Sar-LPFFD-NH <sub>2</sub>	Active	
<i>iAβ5p-A1</i>	Ac-LP-(NMe)FFD-NH <sub>2</sub>	Active	
<i>iAβ5p-A7</i>	Ac-LP-(NMe)F-(NMe)F-(NMe)D-NH <sub>2</sub>	Active	



<i>iAβ5p-A4</i>	Ac-LP-(NMe)F-F-(NMe)D-NH <sub>2</sub>	Active	
<i>iAβ5p-A5</i>	Ac-LP-(NMe)F-(NMe)FD-NH <sub>2</sub>	Active	
<i>iAβ5p-A2</i>	Ac-LPF-(NMe)FD-NH <sub>2</sub>	Active	
<i>iAβ5p-D4</i>	Ac-L-C(ψMe,Mepro)-FFD-NH <sub>2</sub>	Decoys	
<i>iAβ5p-C5</i>	(NMe)Sar-ψ(CH <sub>2</sub> NH)LPFFD-NH <sub>2</sub>	Decoys	
<i>iAβ5p-A3</i>	Ac-LPF-(NMe)F-(NMe)D-NH <sub>2</sub>	Decoys	
<i>iAβ5p-C6</i>	(NMe)-LPFFD-NH <sub>2</sub>	Decoys	

<i>iAβ5p-A6</i>	LP-(NMe)F-(NMe)F-(NMe)D-NH <sub>2</sub>	Decoys	
<i>iAβ5p-D3</i>	Ac-LC-(ψH,Hpro)FFD-NH <sub>2</sub>	Decoys	
<i>iAβ5p-D8</i>	(H)LP-3PyaFD	Inactive	
<i>iAβ5p-D1</i>	(H)L-Ppi-FFD	Inactive	
<i>iAβ5p-D6</i>	(H)LP-HofFD	Inactive	
<i>iAβ5p-C4</i>	Gψ(CH <sub>2</sub> NH)LPFFD-NH <sub>2</sub>	Inactive	
<i>iAβ5p-D7</i>	(H)LP-Na1FD	Inactive	
<i>iAβ5p-D5</i>	(H)-LP-ChaFD	Inactive	

<i>iAβ5p-D2</i>	(H)L-TicFFD	Inactive	
-----------------	-------------	----------	---

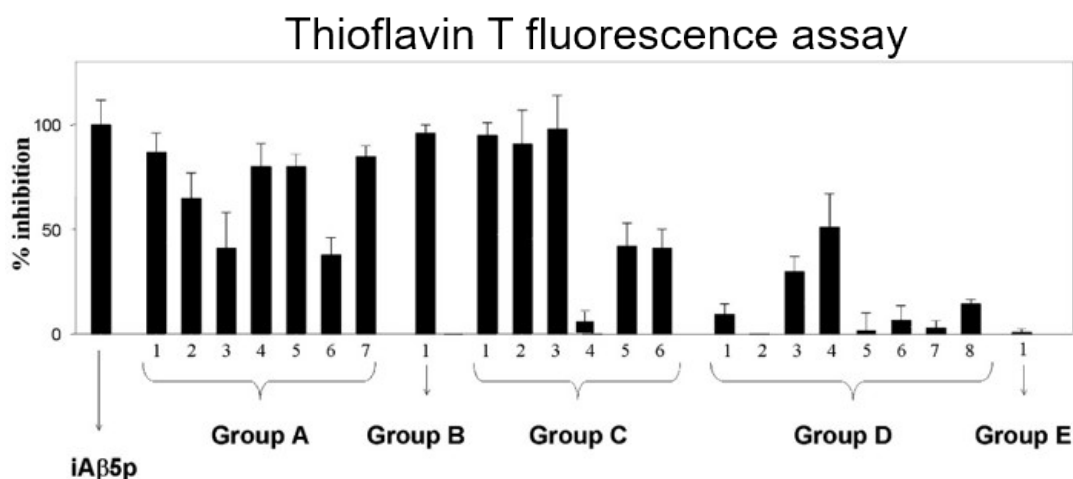


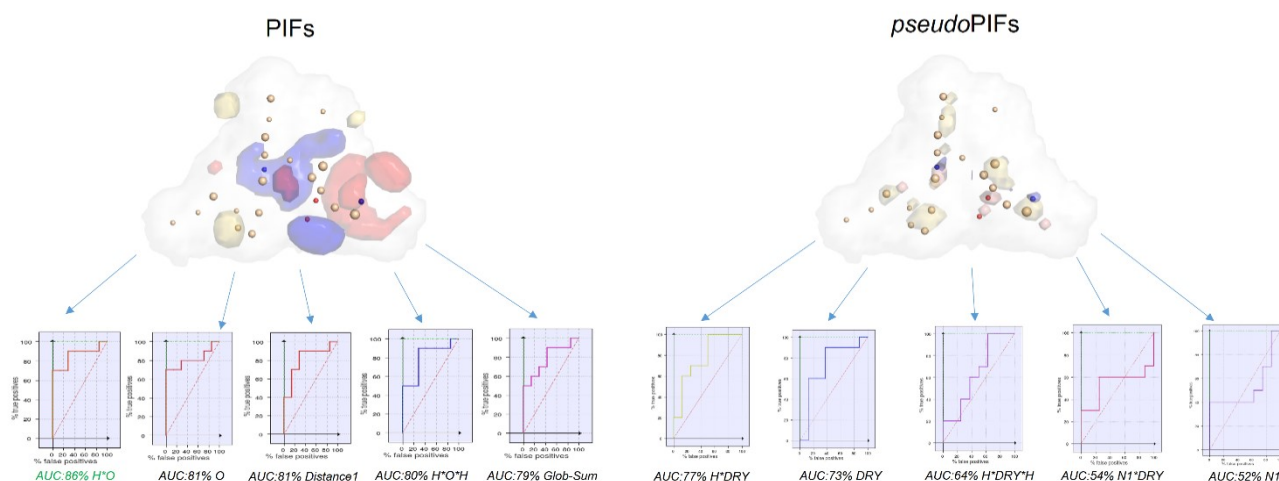
**Figure S10.** Thioflavin T fluorescence assay of BSBPs *iAβ5p* analogs reported in Table S1. Data are taken from the work of Adessi *et al.* 2003 [1]

#### Text S1. FLAPPharm alignment generation.

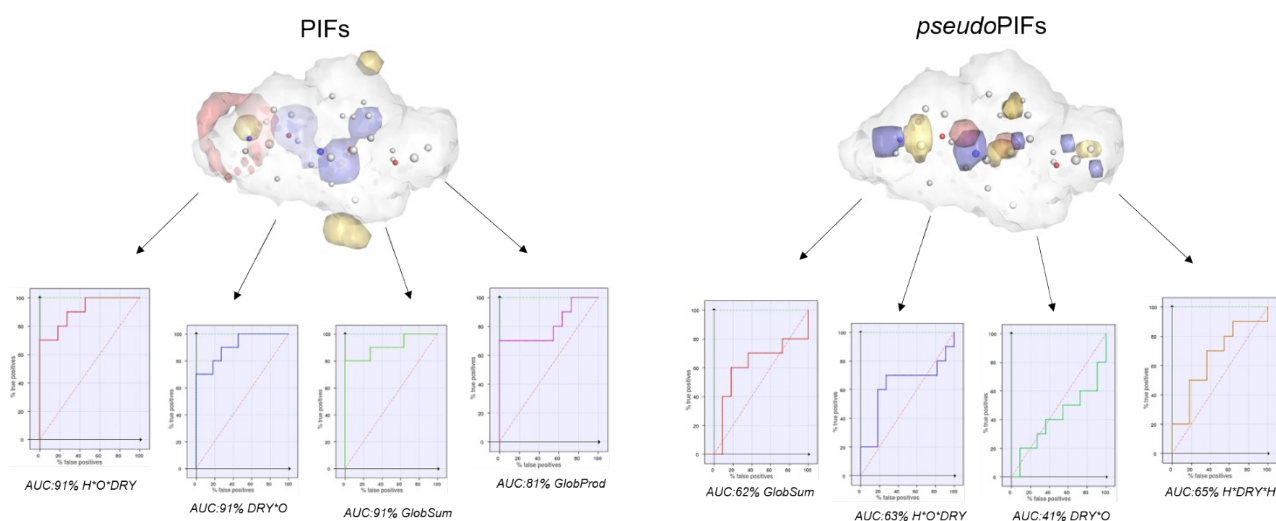
The 3D structure of each known BSBPs collected from literature [1] (Table S1) was built using the Maestro GUI [2] using the X-Ray structure of segment KLVFFA from the  $A\beta_{16-21}$  peptide (PDB ID: 2Y2A) as template [3]. Appropriate structural changes were made to obtain the proper peptides reported in Table S1 and, subsequently, each peptide was treated with Protein Preparation Wizard tool [4] to add missing hydrogen atoms and fix the correct bond order. Peptides were, then, imported into the FLAP (Fingerprint for Ligand And Protein) database performing a stochastic conformational search, generating 30 conformers for each peptide. Then, the 3D-Pharmacophores of each peptide has been generated with the FLAPPharm algorithm [5] as implemented in the software FLAP ver.2.2.1. According to the FLAPPharm algorithm, the alignment of each conformer was carried out in order to extract the pharmacophore named as “pseudomolecule”, consisting both in the Pharmacophoric Interaction Field (PIF) and the pseudofields (pseudoPIFs). The first refers to the common GRID MIFs (Molecular Interaction Fields) [6] similarity, whereas pseudoPIFs represent the common atom-centered pharmacophoric pseudofields. The default GRID probes H, O, N1, and DRY were used to describe shape, hydrogen bond acceptor, hydrogen bond donor and hydrophobic interactions properties, respectively. No constraints were applied during the pharmacophore generation and the accuracy level was set to high. The *Training set* was automatically aligned by FLAPPharm performing two levels of stochastic search: the first level was obtained with the default parameters by generating 30 conformers for each peptide, while the second level was obtained increasing the number of peptide conformers up to 100. For both levels, five pharmacophore models were generated by FLAPPharm, however among the ten pharmacophores, the two best alignments in terms of S-score value resulted to be the Model1 (S-score: 0.667) and Model2 (S-score: 0.517), respectively for the first and the second stochastic search levels. As previously said, the pharmacophore generated by FLAPPharm is described as a ‘pseudomolecule’ composed both by PIFs and pseudoPIFs. Thus, a validation step of both PIFs and pseudoPIFs templates was performed to evaluate the discriminatory power of the two pseudomolecules (Text S2 and Figures S10-S11).

## Text S2. FLAPpharm validation procedure.

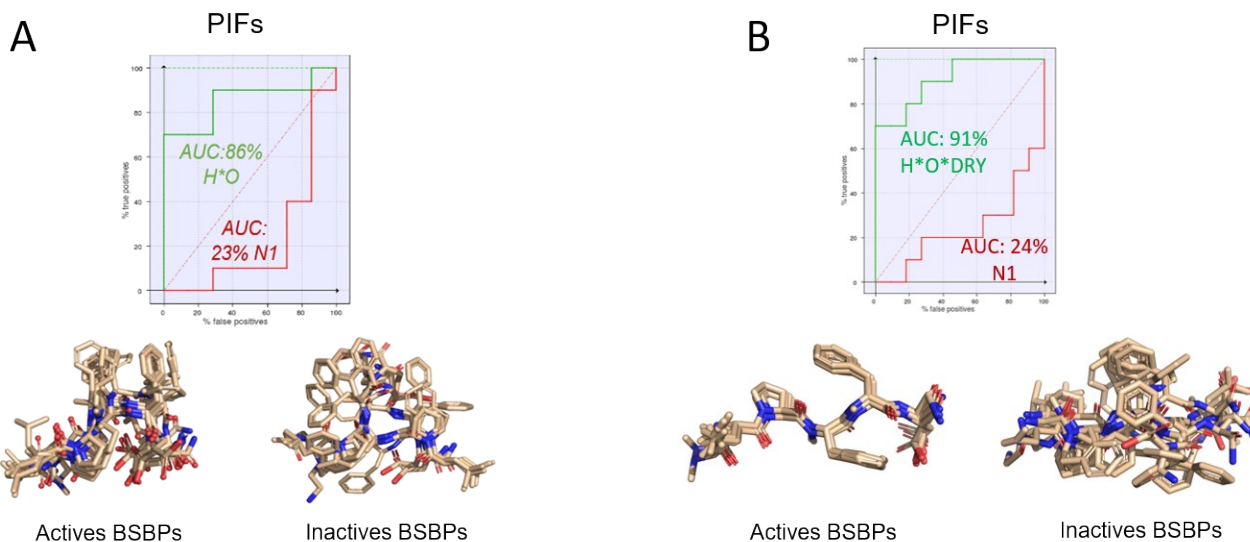
The validation step of both PIFs and *pseudoPIFs* by Enrichment plots are reported in Figures S2 and S3 for Model1 and Model2, respectively. In both Model1 and Model2, the best performance was given by the common interaction fields (PIFs) descriptors. Specifically, in Model1, among the 19 FLAP descriptors, the combination of the H (shape) and O (hydrogen bond acceptor) probes (H\*O) displayed the highest AUC value of 86% with respect to the worst N1 probe with an AUC value of 23% (Figure S11, left panel). On the contrary, in Model2 the H\*O\*DRY descriptor showed the highest AUC value of 91% with respect the worst N1 of 24% (Figure S12, left panel). The quality of the screening can be evaluated also from the good and bad superposition of the active and inactive BSBPs against the template PIF pharmacophore (Figures S13A-B, respectively).



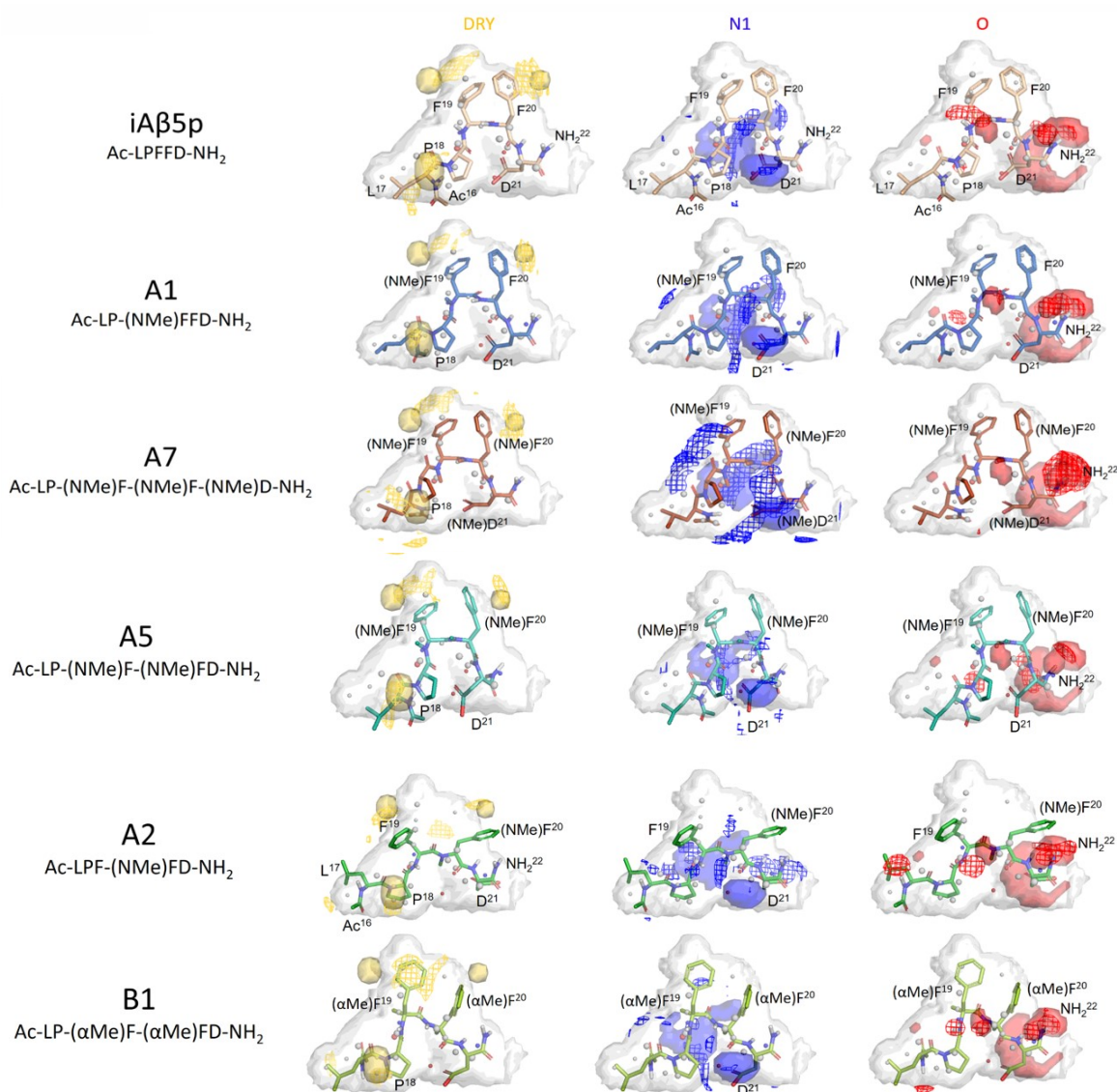
**Figure S11.** The validation step of the two pseudomolecules (PIFs and *pseudoPIFs*) of Model1 by means of the Enrichment plots. From the AUC values it can be observed the better performance of the PIFs pseudomolecule with respect the *pseudoPIFs*. Interestingly, the best similarity of the PIFs pseudomolecule were obtained combining H (Shape) and O (Hydrogen-bond acceptor) probes to give the H\*O descriptor, with an AUC value of 86%. A good performance was observed also with the O probe.



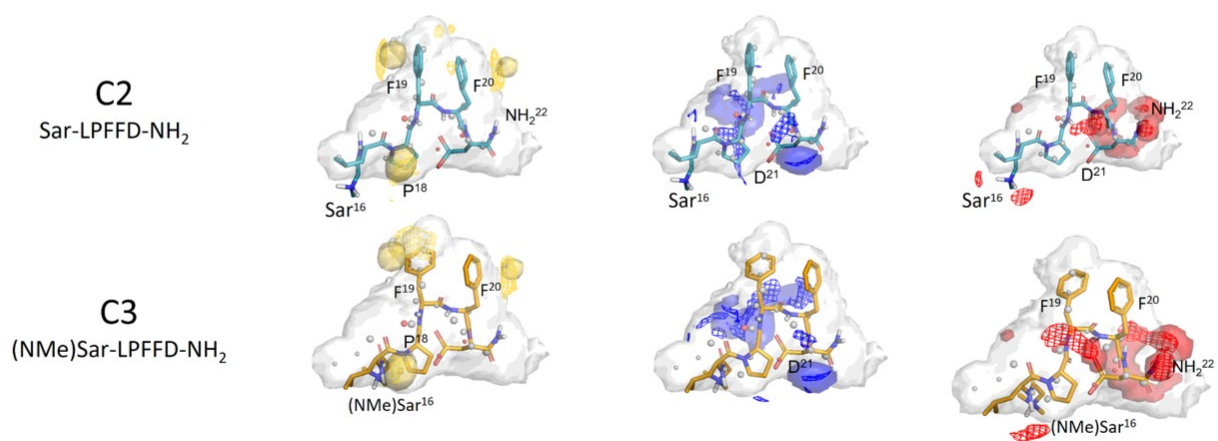
**Figure S12.** The validation step of the two pseudomolecules (PIFs and *pseudoPIFs*) of Model2 by means of the Enrichment plots. From the AUC values it can be observed the better performance of the PIFs pseudomolecule with respect the *pseudoPIFs*. Interestingly, the best similarity of the PIFs pseudomolecule were obtained with the GlobSum descriptor with an AUC value of 91%, even if a good performance was retrieved also with the DRY\*O, the H\*O\*DRY and the GlobProd descriptors.



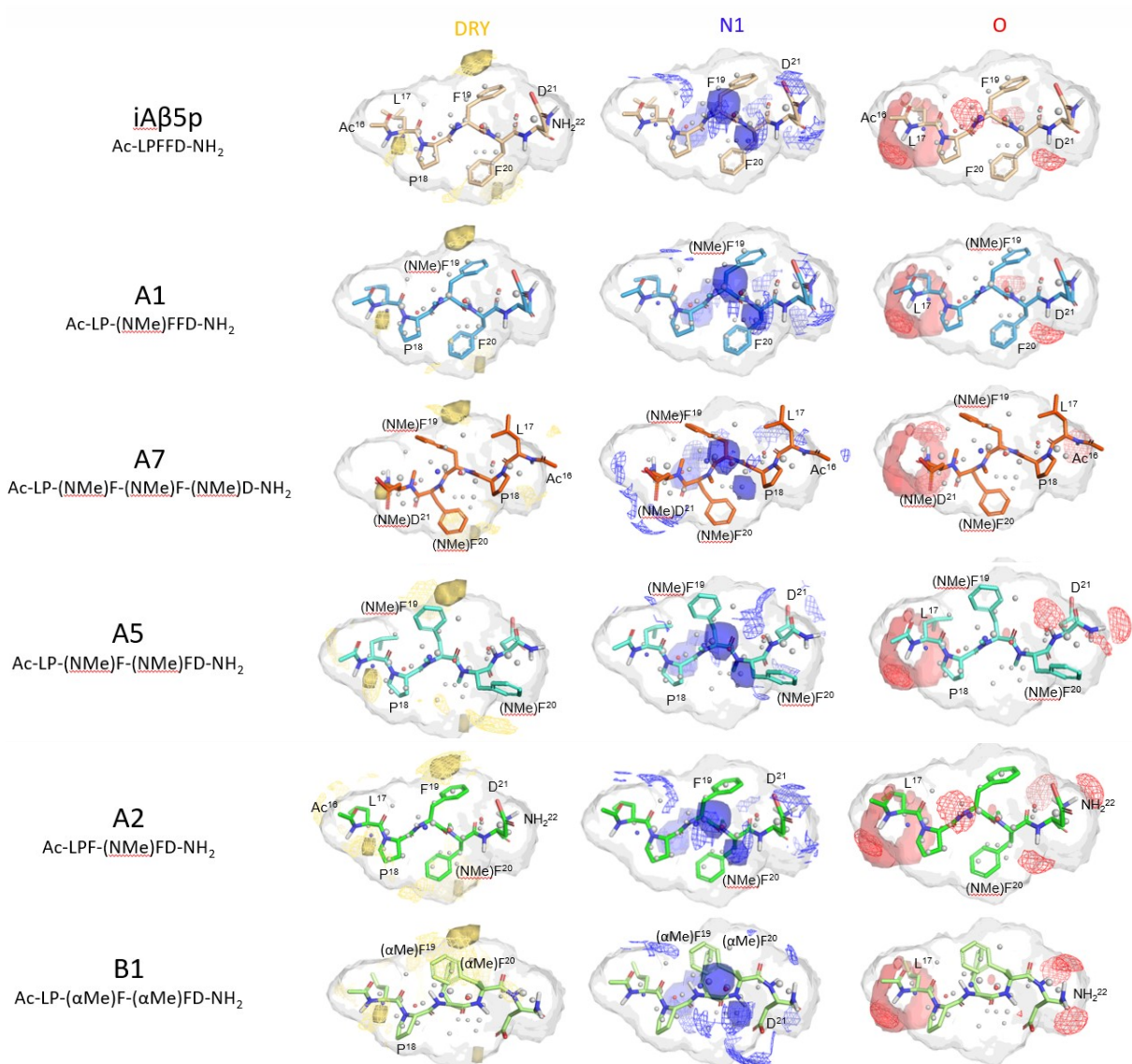
**Figure S13.** Training set alignment on the (A) Model1 PIFs pseudomolecule and (B) Model2 PIFs pseudomolecule, considering the H\*O and H\*O\*DRY descriptors, respectively. The discrimination power of the two pseudomolecules can be observed not only from the best AUC values, but also from the good and bad alignment between the active and inactive BSBPs, respectively.







**Figure S14.** Alignment between MIFs of the most active BSBPs (wireframes) and the PIFs of Model11 (solid transparent surface).



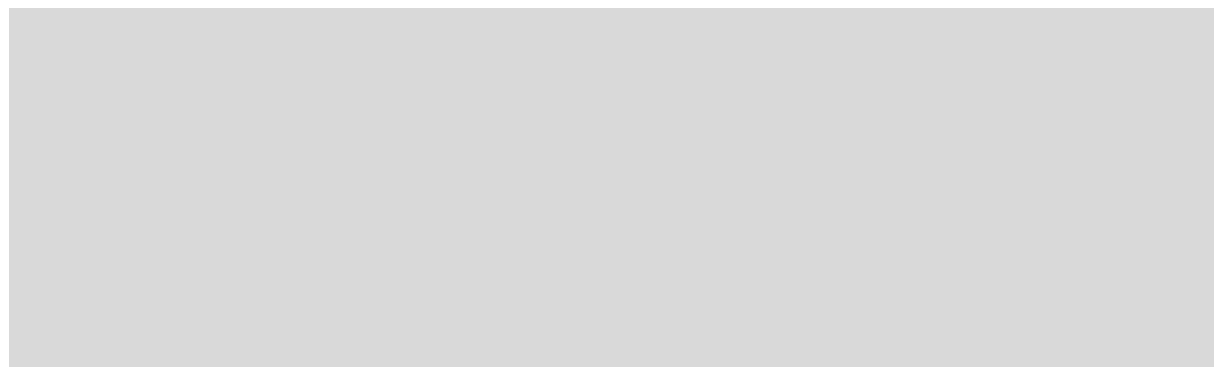


**Figure S15.** Alignment between MIFs of the most active BSBPs (wireframes) and the PIFs of Model2 (solid transparent surface).

**Table S2.** Probe similarity scores of the active (A) and inactive (I) iA $\beta$ 5p analogs from the PIFs screening of Model1. Peptides are ranked for H\*O descriptor.

BSBPs	Active (A) / Inactive (I)		H	N1	DRY	O	H*O	Distance_1	H*O*H	Glob-Sum
	A	I								
A1	A		0.626	0.035	0.024	0.237	0.370	14.517	0.218	0.867
A5	A		0.594	0.036	0.017	0.257	0.363	14.781	0.186	0.785
A7	A		0.601	0.035	0.020	0.260	0.350	14.899	0.164	0.731
iA $\beta$ 5p	A		0.592	0.035	0.017	0.171	0.283	15.000	0.162	0.737
B1	A		0.589	0.039	0.018	0.186	0.282	15.028	0.128	0.671
C2	A		0.637	0.038	0.039	0.128	0.282	14.644	0.176	0.812
A2	A		0.541	0.032	0.031	0.160	0.268	15.146	0.122	0.630
D5	I		0.614	0.041	0.025	0.127	0.268	14.991	0.151	0.718
D7	I		0.572	0.040	0.017	0.138	0.262	15.131	0.131	0.673
A4	A		0.594	0.036	0.019	0.148	0.251	15.119	0.118	0.640
C3	A		0.566	0.038	0.021	0.101	0.235	15.179	0.128	0.684
D6	I		0.552	0.037	0.026	0.134	0.232	15.181	0.106	0.619
D1	I		0.548	0.039	0.016	0.122	0.229	15.274	0.108	0.619
D2	I		0.545	0.047	0.016	0.109	0.224	15.259	0.107	0.644
D8	I		0.531	0.033	0.020	0.093	0.208	15.378	0.096	0.567
C1	A		0.550	0.042	0.021	0.060	0.169	15.413	0.084	0.588
C4	I		0.546	0.043	0.015	0.059	0.165	15.424	0.081	0.622

**Table S3.** Probe similarity scores of the active (A) and inactive (I) iA $\beta$ 5p BSBPs analogs from the PIFs screening of Model2. Peptides are ranked for H\*O\*DRY descriptor.

BSBPs	Active (A) / Inactive (I)		H	N1	DRY	O	H*O	H*O*DRY	DRY*O	Distance_1	H*O*H	Glob-Sum
<b>iA<math>\beta</math>5p</b>	A		0.668	0.029	0.026	0.125	0.271	0.035	0.054	14.769	0.178	0.823
<b>A1</b>	A		0.662	0.027	0.017	0.201	0.357	0.030	0.047	14.673	0.226	0.870
<b>A4</b>	A		0.664	0.026	0.017	0.171	0.272	0.027	0.040	14.860	0.174	0.809
<b>A2</b>	A		0.670	0.031	0.019	0.164	0.292	0.025	0.039	14.817	0.155	0.791
<b>A7</b>	A		0.651	0.025	0.018	0.269	0.328	0.023	0.048	14.822	0.169	0.731
<b>C2</b>	A		0.644	0.024	0.026	0.101	0.214	0.022	0.038	15.067	0.126	0.744
<b>C3</b>	A		0.641	0.024	0.019	0.110	0.227	0.020	0.032	15.104	0.125	0.740
<b>D6</b>	I		0.624	0.028	0.014	0.200	0.320	0.016	0.031	14.976	0.164	0.720
<b>A5</b>	A		0.628	0.024	0.016	0.229	0.340	0.014	0.030	14.907	0.172	0.746
<b>B1</b>	A		0.582	0.024	0.012	0.216	0.280	0.013	0.028	15.185	0.151	0.703
<b>D2</b>	I		0.566	0.027	0.012	0.135	0.265	0.013	0.025	15.224	0.137	0.673
<b>C1</b>	A		0.558	0.026	0.018	0.122	0.247	0.011	0.021	15.291	0.125	0.651
<b>C4</b>	I		0.651	0.028	0.017	0.110	0.227	0.010	0.018	15.184	0.106	0.706
<b>D7</b>	I		0.570	0.029	0.015	0.153	0.268	0.010	0.020	15.235	0.126	0.639
<b>D5</b>	I		0.551	0.036	0.020	0.143	0.255	0.010	0.019	15.227	0.130	0.654
<b>D1</b>	I		0.532	0.025	0.018	0.141	0.259	0.009	0.019	15.318	0.125	0.638
<b>D8</b>	I		0.524	0.027	0.018	0.091	0.206	0.008	0.015	15.458	0.098	0.590

**Table S4:** Probe similarity scores of the designed (d) 2-8 peptides and the decoys (D) iA $\beta$ 5p BSBPs analogs from the PIFs screening of Model1. Peptides are ranked for H\*O\*H descriptor.

Peptides	Designed (d) / Decoys (D)		H	N1	DRY	O	H*O	Distance_1	H*O*H	Glob-Sum
<b>iA<math>\beta</math>5p</b>	A		0.592	0.035	0.017	0.171	0.283	15.000	0.162	0.737
<b>A3</b>	D		0.526	0.030	0.009	0.122	0.244	15.442	0.119	0.616
<b>D3</b>	D		0.538	0.030	0.011	0.142	0.248	15.385	0.107	0.580
<b>D4</b>	D		0.562	0.032	0.015	0.181	0.251	15.294	0.101	0.584
<b>C6</b>	D		0.595	0.039	0.017	0.084	0.203	15.330	0.100	0.629
<b>7</b>	d		0.549	0.032	0.024	0.090	0.208	15.384	0.099	0.598
<b>3</b>	d		0.599	0.033	0.017	0.086	0.167	15.364	0.078	0.654
<b>5</b>	d		0.579	0.030	0.028	0.083	0.170	15.296	0.076	0.649
<b>A6</b>	D		0.539	0.033	0.026	0.063	0.166	15.542	0.075	0.576
<b>2</b>	d		0.538	0.031	0.018	0.084	0.170	15.518	0.074	0.575
<b>C5</b>	D		0.473	0.032	0.015	0.083	0.182	15.591	0.073	0.508
<b>4</b>	d		0.524	0.026	0.024	0.087	0.184	15.543	0.072	0.552
<b>8</b>	d		0.486	0.026	0.025	0.080	0.156	15.632	0.069	0.544
<b>6</b>	d		0.522	0.048	0.044	0.046	0.126	15.490	0.045	0.542



**Table S5:** Probe similarity scores of the designed **2-8** peptides and the decoys iAβ5p BSBPs analogs from the PIFs screening of Model2. Peptides are ranked for H\*O\*DRY descriptor.

Peptides	Design d (d) / Decoys (D)	H	N1	DRY	O	H*O	H*O*DRY	DRY*O	Distance_1	Glob-Sum
<b>iAβ5p</b>	A	0.668	0.029	0.026	0.125	0.271	0.035	0.054	14.769	0.823
<b>C5</b>	D	0.545	0.026	0.017	0.107	0.212	0.016	0.031	15.360	0.636
<b>D3</b>	D	0.568	0.022	0.018	0.164	0.254	0.015	0.029	15.238	0.663
<b>A6</b>	D	0.543	0.027	0.015	0.181	0.293	0.012	0.024	15.179	0.667
<b>6</b>	d	0.480	0.032	0.034	0.046	0.141	0.012	0.027	15.633	0.505
<b>A3</b>	D	0.554	0.024	0.014	0.254	0.326	0.011	0.030	15.102	0.676
<b>D4</b>	D	0.558	0.020	0.013	0.125	0.230	0.011	0.025	15.429	0.603
<b>C6</b>	D	0.592	0.031	0.017	0.105	0.220	0.008	0.015	15.292	0.629
<b>2</b>	d	0.519	0.023	0.022	0.039	0.142	0.006	0.015	15.694	0.552
<b>7</b>	d	0.565	0.020	0.010	0.124	0.198	0.005	0.010	15.538	0.593
<b>4</b>	d	0.533	0.019	0.016	0.091	0.151	0.005	0.011	15.634	0.545
<b>3</b>	d	0.532	0.022	0.012	0.060	0.144	0.005	0.011	15.735	0.541
<b>5</b>	d	0.524	0.022	0.019	0.048	0.135	0.005	0.012	15.721	0.532
<b>8</b>	d	0.431	0.020	0.010	0.093	0.180	0.005	0.015	15.795	0.474

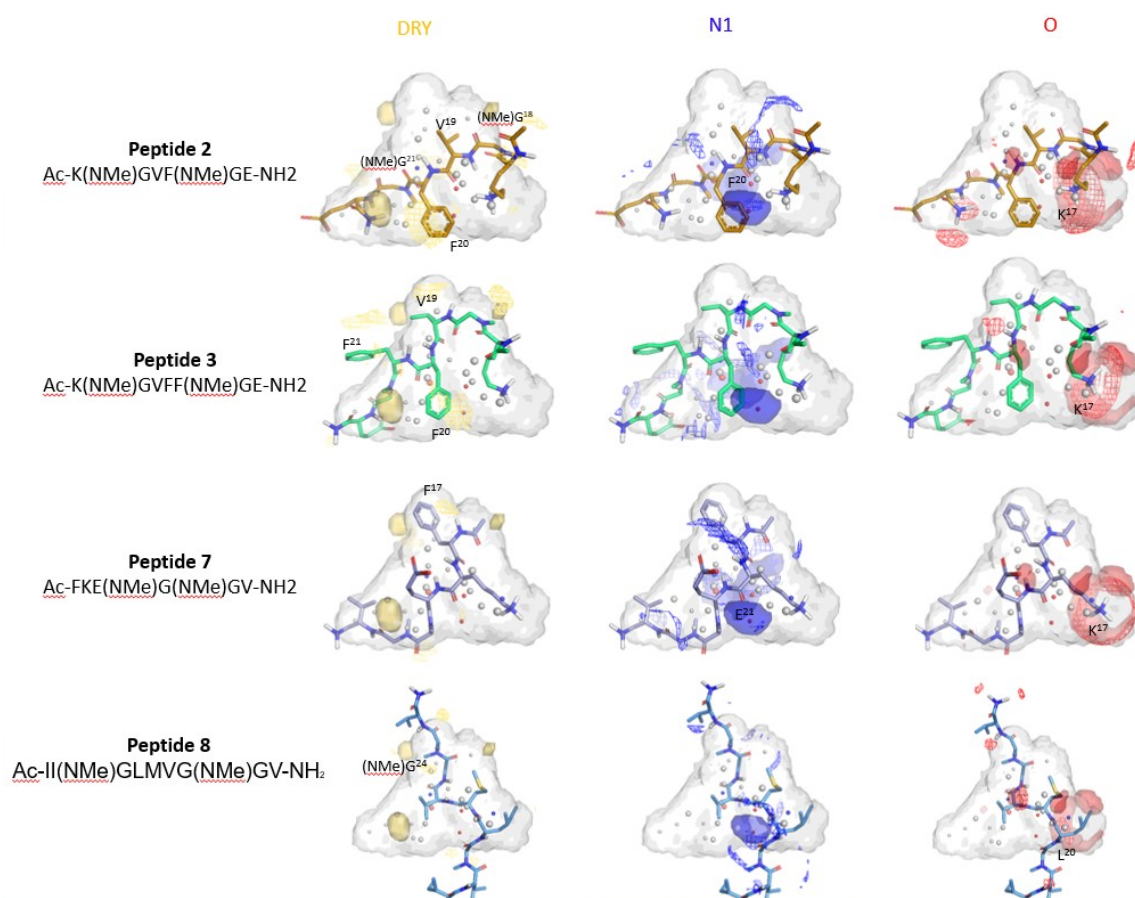


**Figure S16.** Screening results of peptides **2**, **3**, **7** and **8** against the PIF pseudomolecules of Model1, with the overlaps area between their N1, O and DRY MIFs (wireframes) and template MIFs (solid transparent surface).

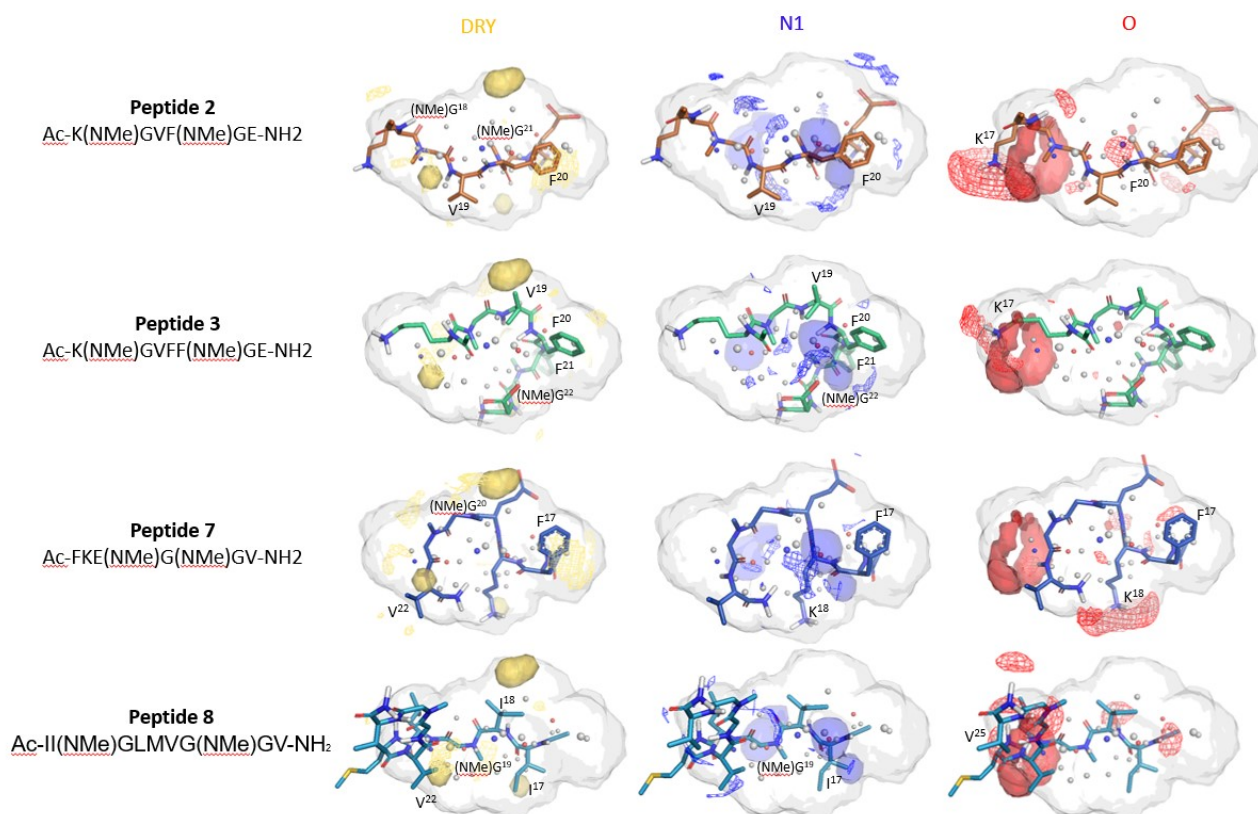


**Figure S17.** Screening results of peptides **2**, **3**, **7** and **8** against the PIF pseudomolecules of Model2, with the overlaps area between their N1, O and DRY MIFs (wireframes) and MIFs template (solid transparent surface).

### Text S3. PT-WTE simulations

The conformational space of the wild-type  $iA\beta 5p$  and the designed peptides **2** and **3** was explored using enhanced sampling methods like Metadynamics (MetaD) to accelerate the sampling process [7]. In MetaD simulations, one chooses a reaction coordinate or collective variables (CVs) along which the system can be biased. History-dependent positive Gaussian hills are then added to the free energy profile along the chosen CV throughout the simulation until a flat free energy profile is obtained. In the well-tempered MetaD variant [8], the bias deposition rate decreases over simulation time by rescaling the Gaussian height  $W$  according to the following eq.1:

$$W = \omega_0 \tau_G e^{-\frac{V_G(S,t)}{k_B \Delta T}} \quad (\text{eq. 1})$$

where  $\tau_G$  is the Gaussian deposition stride,  $\Delta T$  a temperature and  $V_G(S, t)$  is the bias potential accumulated in  $S$  over the time  $t$ , leading the free energy  $F_{(S)}$  to converge as eq. 2:

$$V_G(S, t \rightarrow \infty) = -\frac{\Delta T}{\Delta T + T} F_{(S)} \quad (\text{eq. 2})$$

In some cases, it is useful to use also Replica Exchange Methods (REM) [9], in which the sampling is accelerated by modifying the original Hamiltonian of the system. This is achieved by simulating  $N$  non-interacting replicas of the system at increasing temperature and, at fixed intervals, an exchange configuration between replicas is attempted. One popular case of REM is combining Parallel-tempering (PT) [10] with Well-Tempered Ensemble (WTE), called PT-WTE, which enhances the potential energy fluctuations, thus facilitating replica exchange processes. This also favors exploring low probability regions and overcoming large barriers [11].

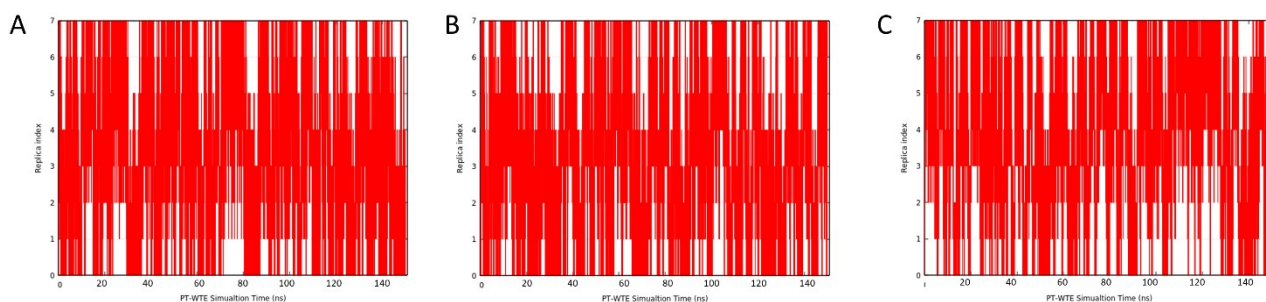


**Figure S18.** Replicas diffusion in temperature (300 K to 450 K) during 150 ns of PT-WTE simulation for (A) iA $\beta$ 5p (B) peptide 2 and (C) peptide 3.

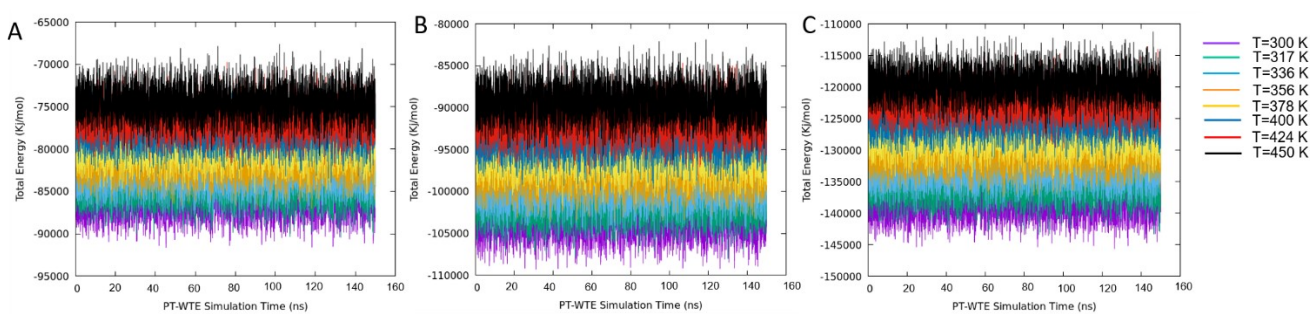


**Figure S19.** Total energy fluctuations at the different temperatures during 150 ns of PT-WTE simulation of (A) iA $\beta$ 5p (B) peptide 2 and (C) peptide 3.

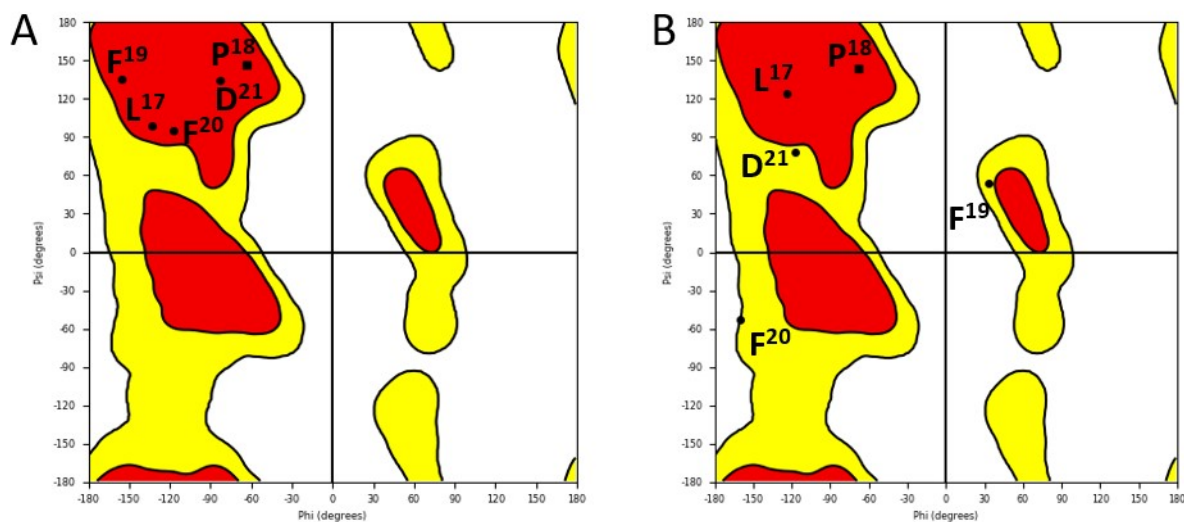


**Figure S20.** Ramachandran plot of the best clustered conformation of iA $\beta$ 5p found by PT-WTE simulation (A) in basin A; (B) in basin B.

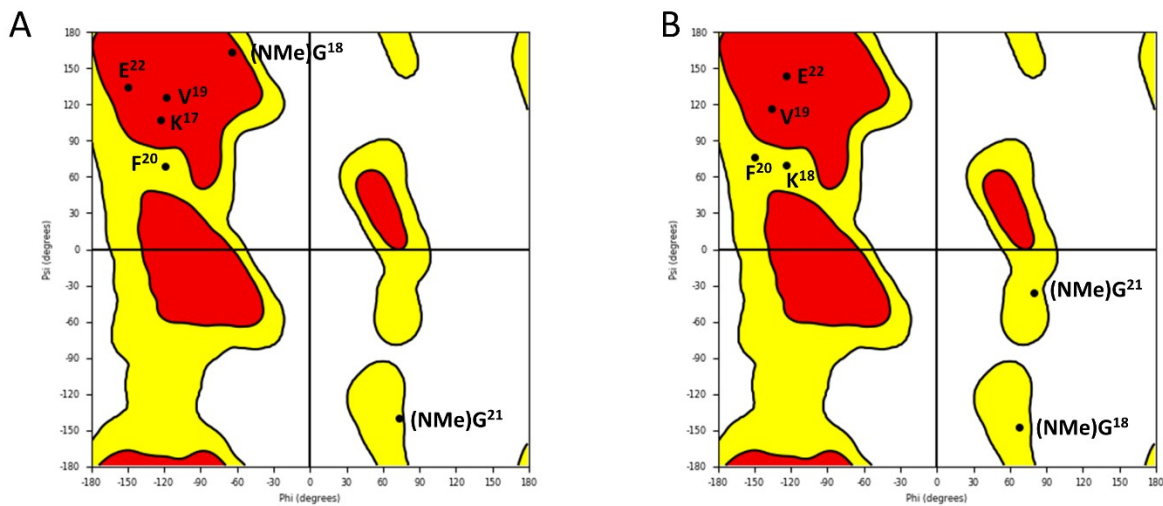


**Figure S21.** Ramachandran plot of the best clustered conformation of peptide **2** found by PT-WTE simulation (A) in basin A and (B) in the energetically-high area B.

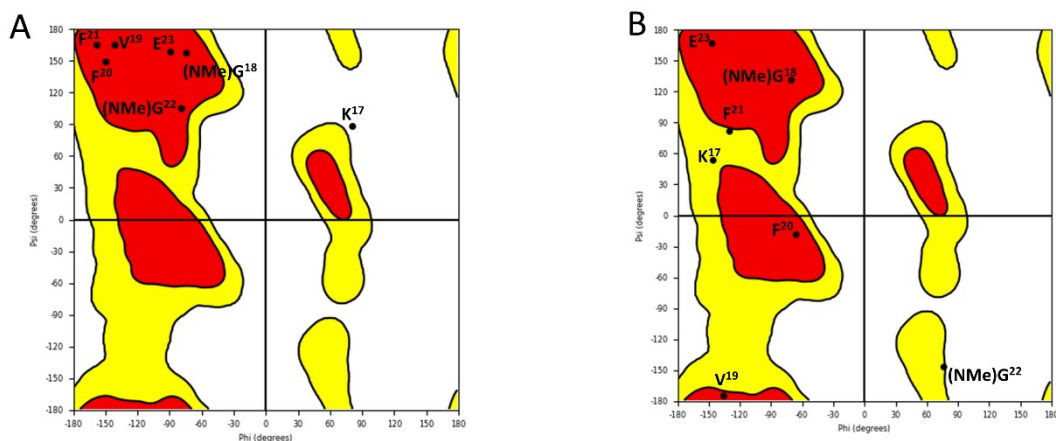


**Figure S22.** Ramachandran plot of the best clustered conformation of peptide **3** found by PT-WTE simulation (A) in basin A and (B) in the energetically-higher basin B.

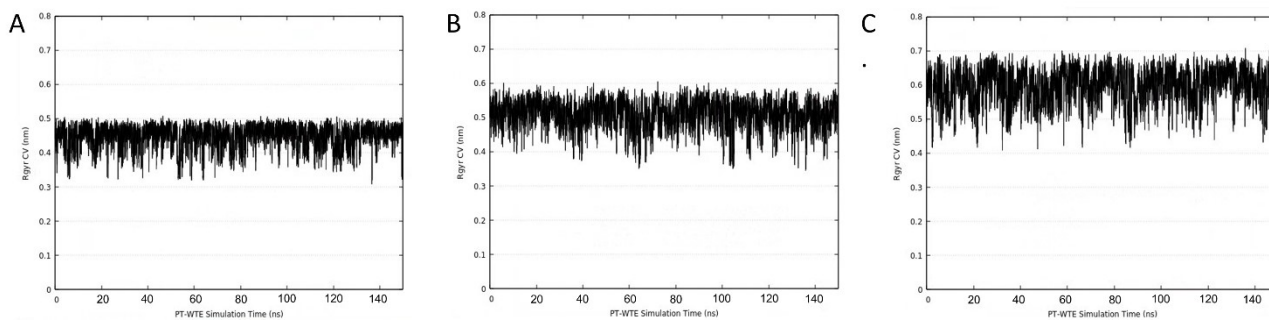


**Figure S23.** Trend of the radius of gyration ( $R_{gry}$ ) CV during 150 ns of PT-WTE simulation of (A) iA $\beta$ 5p (B) peptide **2** and (C) peptide **3**. The  $R_{gry}$  CV was defined by all the Ca atoms.



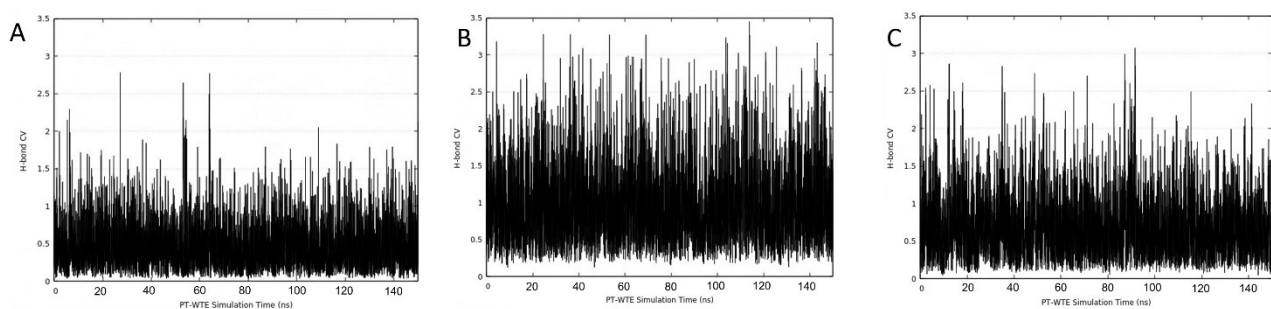


**Figure S24.** Trend of the backbone hydrogen bonds (H-bonds) CV during 150 ns of PT-WTE simulation of (A) iA $\beta$ 5p (B) peptide 2 and (C) peptide 3. The H-bond CV was defined on the backbone O atoms (as acceptor groups) and the backbone N atoms (as donor groups).

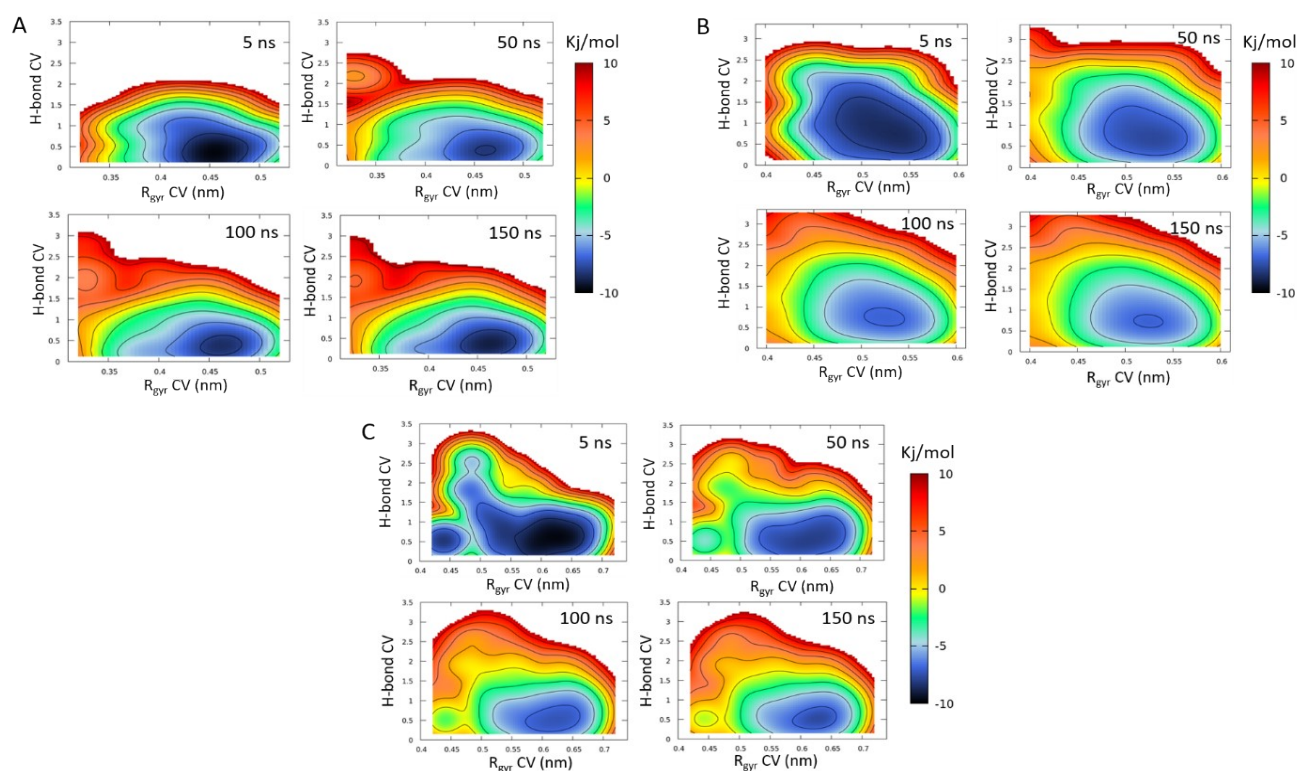


**Figure S25.** FES evolution over simulation time of (A) iA $\beta$ 5p; (B) peptide 2; (C) peptide 3. It can be clearly observed that in the last 50 ns of PT-WTE simulation the Free Energy does not significantly change, thus leading to a convergence.

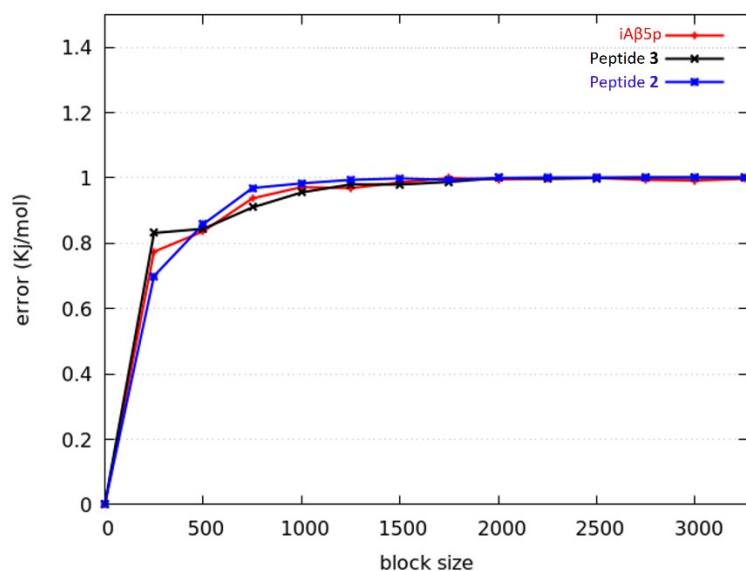
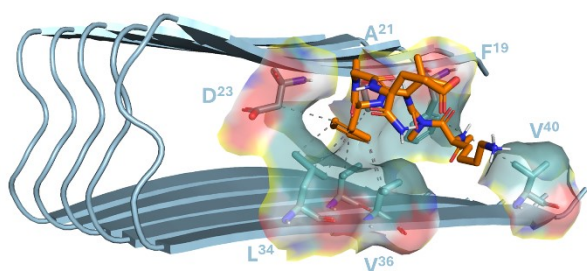
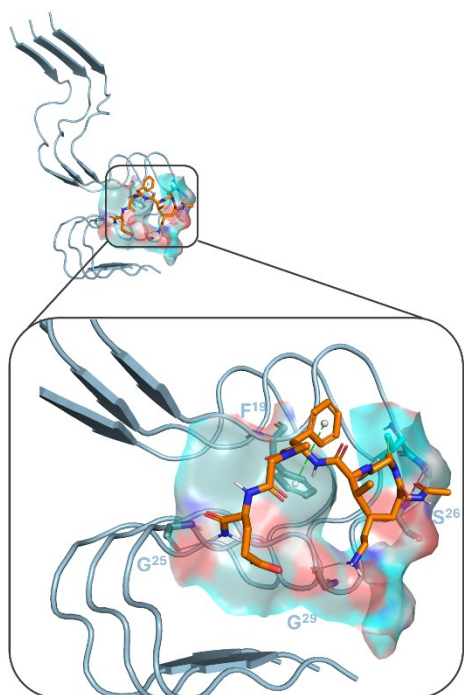


**Figure S26.** Block analysis carried out on the PT-WTE trajectory. The plot shows how the average error on the estimate of the free energy is independent of the block size. In particular, the error bar is smaller when the block sizes are small. As the block sizes get larger, the size of the error bar reaches a plateau to a near constant value.



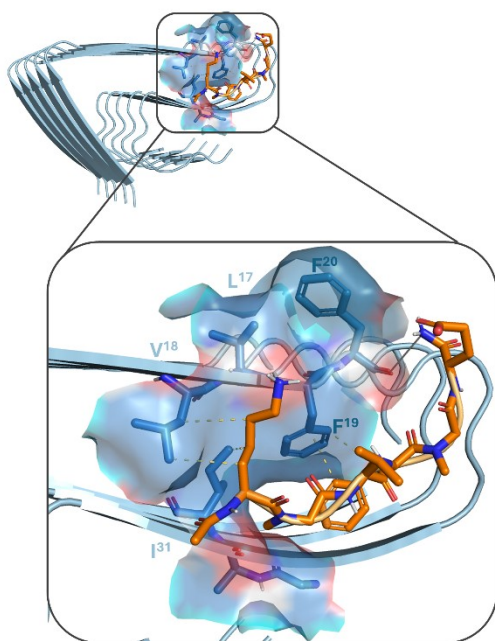
N. Interactions	A $\beta_{(1-42)}$ (2BEG)	Peptide 2	Type of interaction	Distance (Å)
1	F <sup>19</sup>	Ac <sup>16</sup>	Hydrophobic	3.59
1	A <sup>21</sup>	F <sup>20</sup>	Hydrophobic	3.56
1	A <sup>21</sup>	V <sup>19</sup>	Hydrogen bond	2.4
1	D <sup>23</sup>	F <sup>20</sup>	Hydrophobic	3.98
3	L <sup>34</sup>	F <sup>20</sup>	Hydrophobic	3.70
4	L <sup>34</sup>	F <sup>20</sup>	Hydrophobic	3.65

**Figure S27.** (Left) Blind docking best pose of peptide 2 (orange sticks) against the U-shaped solution-NMR structure A $\beta_{(1-42)}$  fibril (PDB ID: 2BEG) (cyan cartoon). (Right) Table of the PLIP tool (Protein Interaction Ligand Profiler) highlighting the main interaction residues involved.



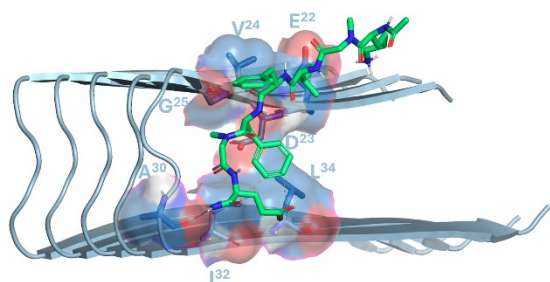
N. Interactions	A $\beta_{(1-42)}$ (2NAO)	Peptide 2	Type of interaction	Distance (Å)
1	F <sup>19</sup>	F <sup>20</sup>	Hydrophobic	3.38
1	F <sup>19</sup>	F <sup>20</sup>	$\pi$ -Stacking (T)	4.74
1	V <sup>24</sup>	(NMe)G <sup>18</sup>	Hydrophobic	3.1
1	G <sup>25</sup>	-Ac <sup>16</sup>	Hydrogen bond	2.80
1	S <sup>26</sup>	-Ac <sup>16</sup>	Hydrogen bond	3.00
1	G <sup>29</sup>	K <sup>17</sup>	Hydrogen bond	2.90
2	G <sup>33</sup>	-NH <sub>2</sub> <sup>23</sup>	Hydrogen bond	3.20

**Figure S28.** (Left) Blind docking best pose of peptide 2 (orange sticks) against the S-shaped solution-NMR structure A $\beta_{(1-42)}$  fibril (PDB ID: 2NAO) (cyan cartoon). (Right) Table of the PLIP tool (Protein Interaction Ligand Profiler) highlighting the main interaction residues involved.



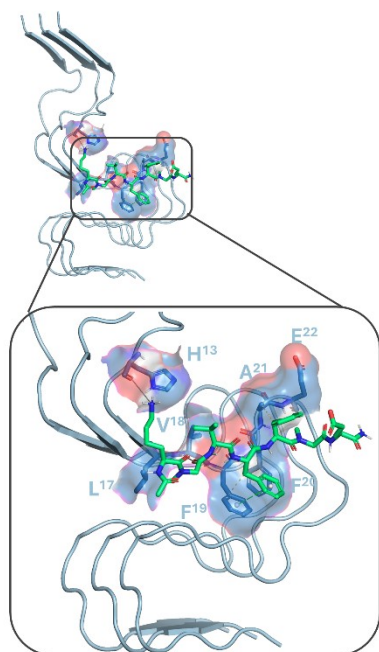
N. Interactions	A $\beta_{(1-42)}$ (5OQV)	Peptide 2	Type of interaction	Distance (Å)
2	L <sup>17</sup>	K <sup>17</sup>	Hydrophobic	3.75
1	I <sup>31</sup>	K <sup>17</sup>	Hydrophobic	3.70
1	V <sup>18</sup>	K <sup>17</sup>	Hydrogen bond	3.20
2	F <sup>19</sup>	F <sup>20</sup>	Hydrophobic	3.40
1	F <sup>20</sup>	-NH <sub>2</sub> <sup>23</sup>	Hydrogen bond	3.50

**Figure S29.** (Left) Blind docking best pose of peptide 2 (orange sticks) against the LS-shaped Cryo-EM structure A $\beta_{(1-42)}$  fibril (PDB ID: 5OQV) (cyan cartoon). (Right) Table of the PLIP tool (Protein Interaction Ligand Profiler) highlighting the main interaction residues involved.



N. Interactions	A $\beta_{(1-42)}$ (2BEG)	Peptide 3	Type of interaction	Distance (Å)
1	E <sup>22</sup>	V <sup>19</sup>	Hydrophobic	3.32
2	I <sup>32</sup>	F <sup>21</sup>	Hydrophobic	3.60
1	L <sup>34</sup>	F <sup>21</sup>	Hydrophobic	3.72
1	G <sup>25</sup>	F <sup>20</sup>	Hydrogen bond	2.8
1	A <sup>30</sup>	-NH <sub>2</sub> <sup>23</sup>	Hydrogen bond	2.5

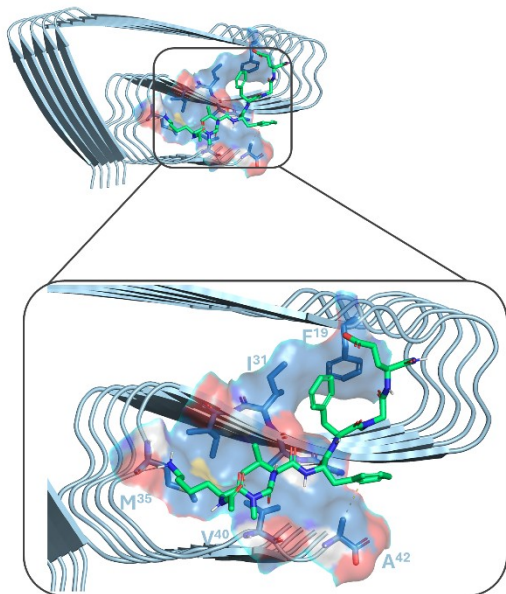
**Figure S30.** (Left) Blind docking best pose of peptide **3** (light-green sticks) against the U-shaped solution-NMR structure A $\beta_{(1-42)}$  fibril (PDB ID: 2BEG) (cyan cartoon). (Right) Table of the PLIP tool (Protein Interaction Ligand Profiler) highlighting the main interaction residues involved.



N. Interactions	A $\beta_{(1-42)}$ (2NAO)	Peptide 3	Type of interaction	Distance (Å)
1	F <sup>19</sup>	F <sup>20</sup>	Hydrophobic	3.77
1	F <sup>20</sup>	F <sup>20</sup>	Hydrophobic	3.50
1	A <sup>21</sup>	F <sup>21</sup>	Hydrophobic	3.95
1	H <sup>13</sup>	K <sup>17</sup>	Hydrogen bond	3.43
1	V <sup>18</sup>	(NMe)G <sup>18</sup>	Hydrogen bond	2.81
1	F <sup>19</sup>	F <sup>20</sup>	Hydrogen bond	3.03
1	F <sup>19</sup>	F <sup>20</sup>	$\pi$ -Stacking (P)	3.96

**Figure S31.** (Left) Blind docking best pose of peptide **3** (light-green sticks) against the S-shaped solution-NMR structure A $\beta_{(1-42)}$  fibril (PDB ID: 2NAO) (cyan cartoon). (Right) Table of the PLIP tool (Protein Interaction Ligand Profiler) highlighting the main interaction residues involved.





N. Interactions	A $\beta_{(1-42)}$ (2NAO)	Peptide 3	Type of interaction	Distance (Å)
1	F <sup>19</sup>	F <sup>21</sup>	Hydrophobic	3.76
1	V <sup>40</sup>	F <sup>20</sup>	Hydrophobic	3.62
1	A <sup>42</sup>	F <sup>20</sup>	Hydrophobic	3.68
1	A <sup>30</sup>	F <sup>20</sup>	Hydrogen bond	3.07
1	M <sup>35</sup>	K <sup>17</sup>	Hydrogen bond	2.88
1	V <sup>40</sup>	(NMe)G <sup>18</sup>	Hydrogen bond	3.52

**Figure S32.** (Left) Blind docking best pose of peptide **3** (light-green sticks) against the LS-shaped Cryo-EM structure A $\beta_{(1-42)}$  fibril (PDB ID: 5OQV) (cyan cartoon). (Right) Table of the PLIP tool (Protein Interaction Ligand Profiler) highlighting the main interaction residues involved.

## References

- [1] Adessi, C.; Frossard, M.J.; Boissard, C.; Fraga, S.; Bieler, S.; Ruckle, T. Pharmacological profiles of peptide drug candidates for the treatment of Alzheimer's disease. *J. Biol. Chem.* **2003**, *278*, 13905–13911. doi:10.1074/jbc.M211976200
- [2] Maestro version 11.1, Schrödinger LLC, New York, NY, 2017.
- [3] Colletier, J.-P.; Laganowsky, A.; Landau, M.; Zhao, M.; Soriaga, A.B.; Goldschmidt, L. Molecular basis for amyloid- $\beta$  polymorphism. *Proc. Natl. Acad. Sci.* **2011**, *108*, 16938–16943. doi:10.1073/PNAS.1112600108
- [4] Madhavi Sastry, G.; Adzhigirey, M.; Day, T.; Annabhimoju, R.; Sherman W. Protein and ligand preparation: parameters, protocols, and influence on virtual screening enrichments. *J. Comput. Aided. Mol. Des.* **2013**, *27*, 221–234. doi:10.1007/s10822-013-9644-8
- [5] Cross, S.; Baroni, M.; Goracci, L.; Cruciani, G. GRID-Based Three-Dimensional Pharmacophores I: FLAPpharm, a Novel Approach for Pharmacophore Elucidation. *J. Chem. Inf. Model.* **2012**, *52*, 2587–2598. doi:10.1021/ci300153d
- [6] Goodford, P.J. A Computational Procedure for Determining Energetically Favorable Binding Sites on Biologically Important Macromolecules. *J. Med. Chem.* **1985**, *28*, 849–857. doi:10.1021/jm00145a002
- [7] Laio, A.; Parrinello, M. Escaping free-energy minima. *Proc. Natl. Acad. Sci. USA* **2002**, *99*, 12562–12566. doi: 10.1073/pnas.202427399
- [8] Barducci, A.; Bussi, G.; Parrinello, M. Well-tempered metadynamics: a smoothly-converging and tunable free-energy method. *Phys Rev Lett.* **2008**, *100*, 020603. doi:10.1103/PhysRevLett.100.020603
- [9] Sugita, Y.; Okamoto, Y. Replica-exchange molecular dynamics method for protein folding. *Chem. Phys. Lett.* **1999**, *314*, 141–151. doi:10.1016/S0009-2614(99)01123-9
- [10] Earl, D.J.; Deem, M.W. Parallel tempering: Theory, applications, and new perspectives. *Phys. Chem. Chem. Phys.* **2005**, *7*, 3910–3916. doi:10.1039/b509983h
- [11] Bonomi, M.; Parrinello, M. Enhanced sampling in the well-tempered ensemble. *Phys. Rev. Lett.* **2010**, *104*, 190601. doi:10.1103/PhysRevLett.104.190601